ACS OMEGA

Open Access

http://pubs.acs.org/journal/acsodf

Article

Lignan and Phthalide Derivatives from the Rhizome of *Ligusticum chuanxiong* (*Rhizoma chuanxiong*) and Evaluation of Their *anti*-Xanthine Oxidase Activities

Man-Li Yang, Hao-Dong Yang, Zhi-Shu Tang,* Xiao-Hui Hu, Rui Zhou, Tao-Tao Xue, Kang Ma, Chun Ji, and Hong-Bo Xu*

Cite This: *ACS Omega* 2023, 8, 39855−39864

Read Online

ACCESS | Metrics & More | Article Recommendations | Supporting Information

ABSTRACT: The previous research results showed that the extracts of ethyl acetate of the rhizome of *Ligusticum chuanxiong* (*Rhizoma chuanxiong*) possessed significant antigout effects in model mice. To explore the active ingredients responsible for the effects, phytochemical studies were performed, which led to the isolation of three rare 8′, 9-linked neolignans, ligusticumins A−C (**1**−**3**), together with two novel phthalide-phenylpropanoid heterodimers, ligusticumalides A−B (**4** and **5**). It is noteworthy that **4** possesses an unprecedented 7-styryl phthalide skeleton. The structures and absolute configurations of **1**−**5** were elucidated by one-dimensional (1D) and two-dimensional (2D) NMR spectroscopy and electron-capture detector (ECD) spectroscopic methods. The bioassay results showed that compounds **1**, **2**, **3**, and **5** presented moderate inhibitory activities against xanthine oxidase (XO) and **4** possessed a significant XO inhibitory effect with an IC_{50} value of 93.88 μM. This is the first time to investigate the *anti*-XO active ingredients of *R. chuanxiong*, which provides valuable information for searching for new antigout agents from natural products.

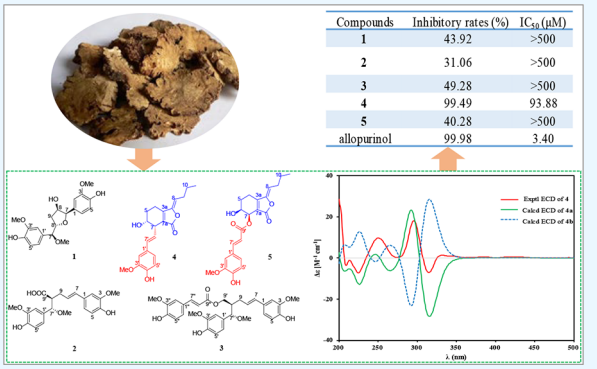

1. INTRODUCTION

The rhizome of *Ligusticum chuanxiong* (*Rhizoma chuanxiong*), also known as "chuan-xiong" in China, is a famous traditional Chinese medicine (TCM). It has been recorded in the "*Shennong Bencaojing*" and is used in TCM to relieve pain and stimulate blood flow.[1,2] Specifically, the herb plant is also commonly used in the treatment of gout in clinical practice in China.[3] Modern pharmacology research has shown that *R. chuanxiong* could prevent and treat arteriosclerosis and dilate blood vessels.[4] In addition, extracts and components obtained from *R. chuanxiong* exhibit a diverse range of activities including antiasthmatic, anti-inflammatory, antimicrobial, antiproliferative, antioxidant, sedative, neuroprotective, and pro-apoptotic effects.[5−7]

Gout is one of the relatively common inflammatory diseases of the joints caused by the deposition of uric acid crystals in the tissues,[8] in which uric acid is produced by xanthine oxidase (XO) acting on the purine bases hypoxanthine and xanthin.[9] In developed countries, the prevalence of gout is 3−6% in males and 1−2% in females, with a strong impact on individual health and healthcare systems.[10] Studies in recent years have shown that gout is an independent risk factor for chronic kidney disease, hypertension, cardiovascular and cerebrovascular diseases, diabetes, and an independent predictor of premature death.[11,12]

Most guidelines available from different regions recommended urate-lowering and/or anti-inflammatory therapies to treat gout.[13] The primary and most prescribed first-line urate-lowering agents are xanthine oxidase (XO) inhibitors, allopurinol, and febuxostat, which reduce the production of uric acid by inhibiting XO.[14] Unfortunately, severe side-effects of allopurinol (hypersensitivity with fever, skin rash and eosinophilia, renal toxicity, gastrointestinal distress) and febuxostat (abnormal liver function tests, headache, gastrointestinal symptoms) hamper their broader therapeutic use and accordingly, there is a need for new potent XO inhibitors with fewer adverse effects.[15,16]

In the initial stage, we first discovered that the methanol extracts of *R. chuanxiong* significantly inhibited XO, with an IC_{50} value of 11.8 μg/mL.[17] Subsequently, Wang et al. also found the same results, and 14 representative compounds (purchased references) of *R. chuanxiong* extracts were tested

Received: August 20, 2023
Accepted: September 21, 2023
Published: October 10, 2023

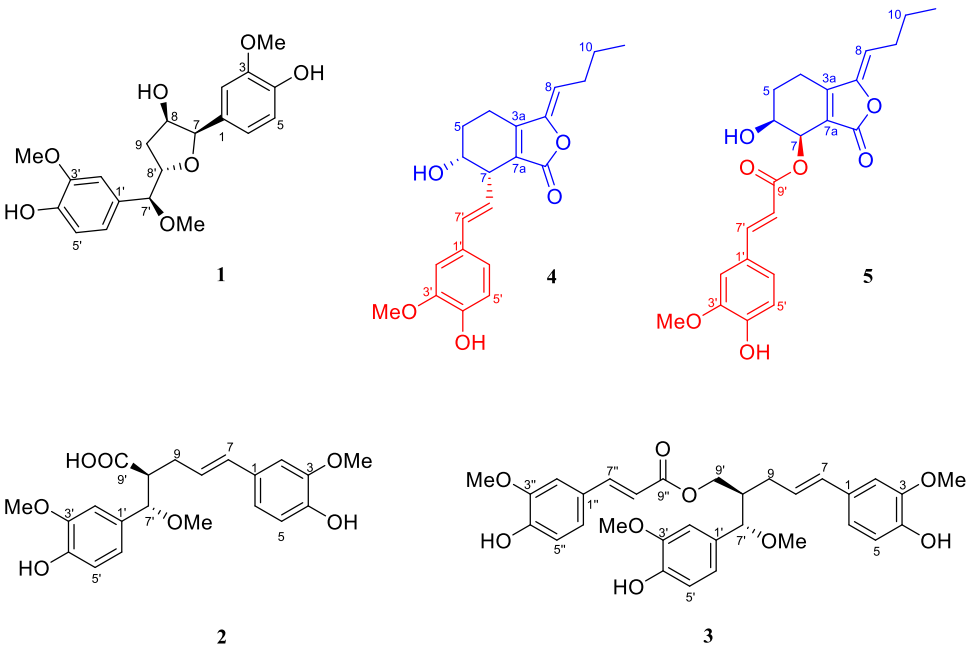

Figure 1. Structures of compounds **1**−**5**.

Table 1. ^{1}H NMR (600 MHz) and ^{13}C NMR (150 MHz) data of 1 (Acetone-d_6), 2 (Methanol-d_4), and 3 (Acetone-d_6) (δ in ppm, J in Hz)

	1		2		3	
no.	δ_H	δ_C	δ_H	δ_C	δ_H	δ_C
1		130.6, C		131.2, C		129.9, C
2	7.00, d (2.0)	111.0, CH	6.83, d (1.8)	110.1, CH	6.97, d (1.9)	108.9, CH
3		147.4, C		149.0, C		147.5, C
4		146.3, C		147.1, C		146.0, C
5	6.76, d (8.0)	114.5, CH	6.81, d (8.0)	116.0, CH	6.73, dd (8.3, 2.0)	114.8, CH
6	6.84, dd (8.0, 2.0)	120.8, CH	6.67, dd (8.0, 1.8)	120.8, CH	6.79, dd (8.4, 2.0)	119.4, CH
7	4.23, d (7.1)	86.5, CH	6.15, d (15.6)	132.9, CH	6.25, d (15.7)	131.7, CH
8	4.40, m	81.2, CH	5.79, m	124.9, CH	6.04, ddd (15.7, 7.8, 1.6)	125.1, CH
9	1.97, ddd (12.0, 6.4, 3.1)	36.8, CH_2	2.21, m	34.1, CH_2	2.23, overlap	31.6, CH_2
	1.72, m		1.98, m		2.14, m	
3-OMe	3.86, s	55.4, CH_3	3.82, s	56.3, CH_3	3.81, s	55.3, CH_3
1′		133.4, C		131.8, C		131.5, C
2′	6.94, d (2.8)	109.2, CH	6.92, d (1.7)	111.8, CH	6.97, d (1.9)	110.5, CH
3′		147.2, C		149.4, C		147.6, C
4′		145.7, C		147.9, C		146.3, C
5′	6.83, d (8.2)	114.5, CH	6.66, d (8.1)	116.1, CH	6.86, overlap	114.6, CH
6′	6.80, dd (8.2, 2.8)	118.4, CH	6.80, dd (8.1, 1.7)	122.2, CH	6.86, overlap	120.5, CH
7′	4.62, d (4.6)	86.5, CH	4.20, d (9.9)	86.7, CH	4.18, d (7.8)	83.3, CH
8′	4.07, m	78.0, CH	2.74, m	55.6, CH	2.23, overlap	44.9, CH
9′				178.9, C	4.32, m	63.2, CH_2
3′-OMe	3.83, s	55.3, CH_3	3.85, s	56.4, CH_3	3.86, s	55.4, CH_3
7′-OMe	3.23, s	56.0, CH_3	3.12, s	56.7, CH_3	3.17, s	55.9, CH_3
1″						126.6, C
2″					7.32, d (1.9)	110.4, CH
3″						147.9, C
4″						149.2, C
5″					6.86, overlap	115.2, CH
6″					7.12, dd (8.3,1.9)	123.1, CH
7″					7.59, d (15.9)	144.7, CH
8″					6.42, d (15. 9)	115.1, CH
9″						166.6, C
3″-OMe					3.92, s	55.5, CH_3

https://doi.org/10.1021/acsomega.3c06172
ACS Omega 2023, 8, 39855−39864

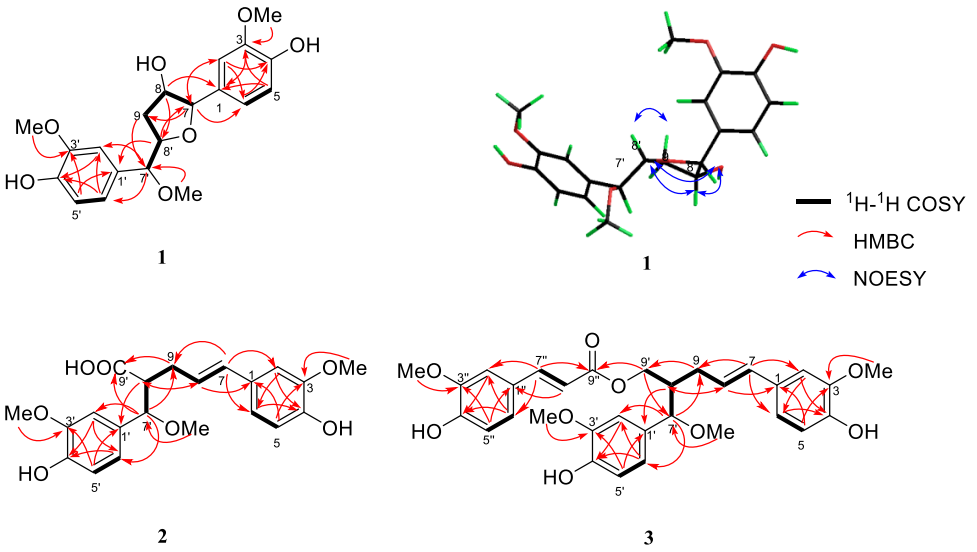

Figure 2. Key two-dimensional (2D) NMR correlations of **1**, **2**, and **3**.

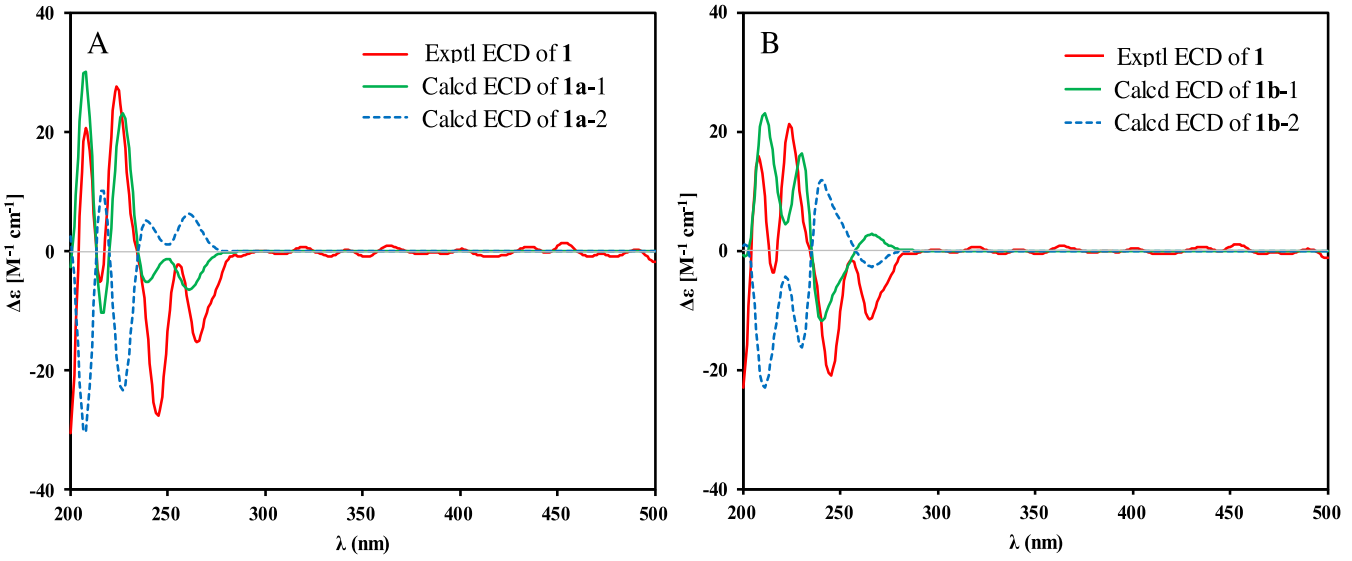

Figure 3. Experimental and calculated ECD spectra of **1a** (A) and **1b** (B).

for their inhibitory effects on XO, of which coniferyl ferulate showed an inhibition ratio of 99.2% at 200 μM.[18] Our further investigations found that ethyl acetate extracts of *R. chuanxiong* showed comparable XO-inhibiting activity (IC_{50} = 18.25 ± 0.19 μg/mL) to the methanol extract. At the same time, this ethyl acetate extract (500 mg/kg) could reduce the serum uric acid level of oxonate potassium-induced hyperuricemic mice by oral administration. Compared with that in the model group, the serum uric acid content decreased by an average of 60.92% in these mice. In addition, oral administration of the same dose of ethyl acetate extracts also significantly reversed the paw swelling of mice with acute gouty arthritis induced by monosodium urate (MSU) crystals, and about 75% inhibition of swelling was observed after 4 h of administration.[19]

The above results suggested that the extracts of ethyl acetate of *R. chuanxiong* possessed potential antigout effects. Herein, we report further research on active ingredients responsible for the effects in *R. chuanxiong*, including the isolation, structure elucidation, and XO inhibitory activities of ligusticumin A (**1**), ligusticumin B (**2**), ligusticumin C (**3**), ligusticumalide A (**4**), and ligusticumalide B (**5**) (Figure 1).

2. RESULTS AND DISCUSSION

2.1. Structural Elucidation. Ligusticumin A (**1**) was obtained as a light yellow powder and determined to have the molecular formula $C_{20}H_{24}O_7$, based on the ion at *m*/*z* 399.1412 $[M + Na]^+$ (calcd. 399.1414) in HR-ESIMS, which corresponds to nine indices of hydrogen deficiency. In accordance with its molecular formula, all 20 carbons were well resolved in the ^{13}C NMR (HSQC) spectrum and identified as three methyls, one methylene, and ten methines including four oxygenated tertiary carbon and six quaternary carbons (Table 1). Three methoxy carbons were revealed based on the signals at δ_C 55.3 (q), 55.4 (q) and 56.0 (q) in the ^{13}C NMR spectrum, along with the characteristic protons at δ_H 3.83 (3H, s), 3.86 (3H, s), and 3.23 (3H, s).

Two *p*-hydroxy-*m*-methoxyphenyls were recognized according to the ^{13}C and ^{1}H NMR data, which was further confirmed by the ^{1}H−^{1}H COSY correlations of H-5 (δ_H 6.76)/H-6 (δ_H

https://doi.org/10.1021/acsomega.3c06172
ACS Omega 2023, 8, 39855−39864

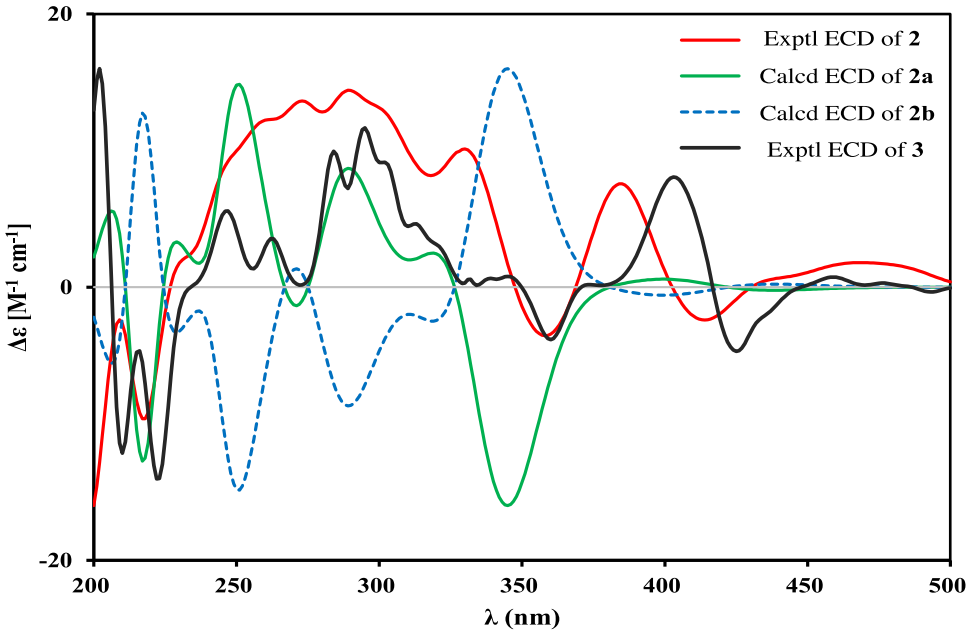

Figure 4. Comparison of the calculated ECD spectra for **2a** and **2b** with the experimental spectra of **2** and **3**.

6.84), and H-5′ (δ_H 6.83)/H-6′ (δ_H 6.80), and the HMBC correlations from H-2 (δ_H 7.00) to C-4 (δ_C 146.3)/C-6 (δ_C 120.8), H-5 (δ_H 6.76) to C-1 (δ_C 130.6)/C-3 (δ_C 147.4), H-6 (δ_H 6.84) to C-4 (δ_C 146.3), methoxy protons (δ_H 3.86) to C-3 (δ_C 147.4), H-2′ (δ_H 6.94) to C-4′ (δ_C 145.7), H-5′ (δ_H 6.83) to C-1′ (δ_C 133.4)/C-3′ (δ_C 147.2), H-6′ (δ_H 6.80) to C-2′ (δ_C 109.2)/C-4′ (δ_C 145.7), and methoxy protons (δ_H 3.83) to C-3′ (δ_C 147.2). In addition, the ^{1}H−^{1}H COSY correlations of H-7 (δ_H 4.23)/H-8 (δ_H 4.40)/H-9 (δ_H 1.72, 1.97)/H-8′ (δ_H 4.07) and HMBC correlations from H-7 (δ_H 4.23) to C-9 (δ_C 36.8), H-8 (δ_H 4.40) to C-8′ (δ_C 78.0), and H-8′ (δ_H 4.07) to C-7 (δ_C 86.5) indicated the presence of a tetrahydrofuran part. The HMBC correlation from methoxy protons (δ_H 3.23) to C-7′ (δ_C 86.5) revealed that one methoxyl group connected at C-7′. The NMR data of H-8 (δ_H 4.40), C-8 (δ_C 81.2), and its molecular formula ($C_{20}H_{24}O_7$) suggested one hydroxy connected at C-8. Moreover, the HMBC correlations from H-7′ (δ_H 4.62) to C-2′ (δ_C 109.2)/C-6′ (δ_C 118.4), H-8′ (δ_H 4.07) to C-1′ (δ_C 133.4), and H-9 (δ_H 1.72, 1.97) to C-7′ (δ_C 86.5), and ^{1}H−^{1}H COSY correlation of H-7′ (δ_H 4.62)/H-8′ (δ_H 4.07) confirmed one *p*-hydroxy-*m*-methoxyphenyl moiety linked with the tetrahydrofuran fragment by C-1′−C-7′−C-8′. The other *p*-hydroxy-*m*-methoxyphenyl linked with the tetrahydrofuran ring through C-1−C-7, which was determined by the HMBC correlations from H-7 (δ_H 4.23) to C-2 (δ_C 111.0)/C-6 (δ_C 120.8), and H-8 (δ_H 4.40) to C-1 (δ_C 130.6). Thus, the planar structure of **1** was determined as a rare norneolignan with tetrahydrofuran moiety (Figure 2).

According to the ROESY correlations of H-7 (δ_H 4.23)/H-8 (δ_H 4.40)/H-9a (δ_H 1.97) and H-8′ (δ_H 4.07)/H-9b (δ_H 1.72) (Figure 2), the relative configurations of C-7, C-8 and C-8′ were assigned as 7*R**, 8*R**, 8′*S**, respectively. Taking into account the two configurations of C-7, the relative configurations of **1** were 7*R**, 8*R**, 7′*S*, 8′*S**(**1a**) or 7*R**, 8*R**, 7′*R*, 8′*S**(**1b**).

Finally, the absolute configuration of **1** was established by comparing its experimental and calculated electron-capture detector (ECD) spectra on four possible structures: (7*R*, 8*R*, 7′*S*, 8′*S*)-**1a** (**1a-1**), (7*S*, 8*S*, 7′*R*, 8′*R*)-**1a** (**1a-2**), (7*R*, 8*R*, 7′*R*, 8′*S*)-**1b** (**1b-1**), and (7*S*, 8*S*, 7′*S*, 8′*R*)-**1b** (**1b-2**). As shown in Figure 3, the calculated weighted ECD spectrum of **1a-1** matched well with the experimental ECD, indicating the absolute configuration of **1** to be 7*R*, 8*R*, 7′*S*, 8′*S*.

The pale yellow oil, ligusticumin B (**2**), was assigned the molecular formula $C_{21}H_{24}O_7$ (10 indices of hydrogen deficiency) by a positive HR-ESIMS ion *m*/*z* 411.1409 [M + Na]$^+$ (calcd. 411.1414). The ^{1}H NMR spectrum displayed three methoxy signals at δ_H: 3.82 (3H, s, 3-OMe), 3.85 (3H, s, 3′-OMe), 3.12 (3H, s, 7′-OMe), and a group of *trans*-C=C proton signals at δ_H: 6.15 (1H, d, *J* = 15.6 Hz, H-7), 5.79 (1H, m, H-8).

The ^{13}C NMR (HSQC) spectra showed 21 carbon resonances, which were ascribed to three methyls, one methylene, ten methines, and seven quaternary carbons including four oxygenated unsaturated carbons (δ_C 149.0, 147.1, 149.4, 147.9) and one carbonyl carbon (δ_C 178.9) (Table 1).

The HMBC correlations from methoxy protons (δ_H 3.82) to C-3 (δ_C 149.0), and methoxy protons (δ_H 3.85) to C-3′ (δ_C 149.4) suggested that the two methoxys connected at C-3 and C-3′, respectively. The ^{1}H−^{1}H COSY correlations of H-5 (δ_H 6.81)/H-6 (δ_H 6.67) and H-7 (δ_H 6.15)/H-8 (δ_H 5.79)/H-9 (δ_H 2.21, 1.98) and the HMBC correlations from H-2 (δ_H 6.83) to C-4 (δ_C 147.1)/C-6 (δ_C 120.8), H-5 (δ_H 6.81) to C-1 (δ_C 131.2)/C-3 (δ_C 149.0), H-6 (δ_H 6.67) to C-4 (δ_C 147.1), H-7 (δ_H 6.15) to C-2 (δ_C 110.1)/C-6 (δ_C 120.8)/C-9 (δ_C 34.1), and H-8 (δ_H 5.79) to C-1 (δ_C 131.2) indicated the presence of one C_6−C_3 unit. In addition, another C_6−C_3 unit was identified by the ^{1}H−^{1}H COSY correlations of H-5′ (δ_H 6.66)/H-6′ (δ_H 6.80) and H-7′ (δ_H 4.20)/H-8′ (δ_H 2.74) and its HMBC correlations from H-2′ (δ_H 6.92) to C-4′ (δ_C 147.9)/C-6′ (δ_C 122.2), H-5′ (δ_H 6.66) to C-1′ (δ_C 131.8)/C-3′ (δ_C 149.4), H-6′ (δ_H 6.80) to C-4′ (δ_C 147.9), H-7′ (δ_H 4.20) to C-2′ (δ_C 111.8)/C-6′ (δ_C 122.2)/C-9′ (δ_C 178.9), H-8′ (δ_H 2.74) to C-1′ (δ_C 131.8), and methoxy protons (δ_H 3.12) to C-7′ (δ_C 86.7). Meanwhile, the ^{1}H−^{1}H COSY correlations of H-9 (δ_H 2.21, 1.98)/H-8′ (δ_H 2.74) and HMBC

https://doi.org/10.1021/acsomega.3c06172
ACS Omega 2023, 8, 39855−39864

correlations from H-9 (δ_H 2.21, 1.98) to C-9′ (δ_C 178.9), H-7′ (δ_H 4.20) to C-9 (δ_C 34.1), and H-8′ (δ_H 2.74) to C-8 (δ_C 124.9) indicated that compound **2** is a rare neolignan, which was generated from two C_6-C_3 phenylpropanoid units linked by C-8′−C-9 (Figure 2).

Previous investigation revealed that compounds with a *threo* form of C-7′ and C-8′ could be distinguished from its *erythro* isomer with the $^3J_{H,H}$ coupling constant of the H-7′/H-8′ protons, which the $J_{7',8'}$ value in the *threo* form (usually greater than 6 Hz) was larger than the *erythro* form (usually less than 6 Hz).[20−22] Thus, the relative configurations of **2** at the C-7′ and C-8′ were assigned as *threo* by the $J_{H\text{-}7',8'}$ value of 9.9 Hz (Table 1).

To establish the absolute configuration of **2**, the ECD spectra of the two possible structures (7′*S*, 8′*S*)-**2** (**2a**) and (7′*R*, 8′*R*)-**2** (**2b**) were calculated by TDDFT methods. As shown in Figure 4, the calculated ECD spectrum of (7′*S*, 8′*S*)-**2** (**2a**) matched well with the experimental one, defining the (7′*S*, 8′*S*) absolute configuration of **2**.

Ligusticumin C (**3**) was obtained as a yellow oil and had a molecular formula of $C_{31}H_{34}O_9$ with 15 degrees of unsaturation based on a quasi-molecular ion peak at *m*/*z* 573.2086 $[M + Na]^+$ (calcd. 573.2095) in HR-ESIMS. The one-dimensional (1D) NMR data exhibited that, compared with **2**, compound **3** presented an additional feruloyl signal, which was confirmed by the $^1H-^1H$ COSY correlations of H-5″ (δ_H 6.86)/H-6″ (δ_H 7.12) and H-7″ (δ_H 7.59)/H-8″ (δ_H 6.42) and the HMBC correlations from H-2″ (δ_H 7.32) to C-4″ (δ_C 149.2), H-5″ (δ_H 6.86) to C-1″ (δ_C 126.6)/C-3″ (δ_C 147.9), H-6″ (δ_H 7.12) to C-2″ (δ_C 110.4)/C-4″ (δ_C 149.2), H-7″ (δ_H 7.59) to C-2″ (δ_C 110.4)/C-6″ (δ_C 123.1)/C-9″ (δ_C 166.6), H-8″ (δ_H 6.42) to C-1″ (δ_C 126.6), and methoxy protons (δ_H 3.92) to C-3″ (δ_C 147.9). Furthermore, the additional feruloyl connects at C-9′ by the HMBC correlation from H-9′ (δ_H 4.32) to C-9″ (δ_C 166.6).

Thus, the planar structure of **3** was fully established (Figure 2), and the assignments of all of the proton and carbon resonances are shown in Table 1. The absolute configurations of **3** were tentatively assigned as 7′*S*, 8′*R* on the basis of its ECD spectrum, and the experimental ECD of **3** was consistent with that of **2** (Figure 4).

To determine the absolute configurations of **3**, the specific rotation of (7′*S*, 8′*R*)-**3** (**3a**) was calculated at the B3LYP/aug-cc-PvDZ level with an IEFPCM model in MeOH (Table S7, Supporting Information). The calculated specific rotation of **3a** was +157.5, which was close to the experimental value $[\alpha]_D^{29}$ +139.2 (*c* 0.065, MeOH).

Ligusticumalide A (**4**) was obtained as an oil and had a molecular formula of $C_{21}H_{24}O_5$ with 10 degrees of unsaturation based on an HR-ESIMS ion peak at *m*/*z* 357.1699 $[M + Na]^+$ (calcd. 357.1697). The ^1H NMR spectrum of compound **4** exhibited signals for one methoxy at δ_H 3.83, one methyl at δ_H 0.96 (t, J = 7.4 Hz), and one oxygenated methine at δ_H 4.05. The ^{13}C NMR (HSQC) spectra showed the resonances of two methyls, four methylenes, eight methines, and seven quaternary carbons (Table 2). Among these, one ester carbonyl carbon (δ_C: 169.0) and two groups of olefinic carbons (δ_C: 148.5, 111.9, 151.1, 125.6) were easily distinguished in the downfield region of ^{13}C NMR spectrum, which suggested that **4** was a derivative of senkyunolide H.[23]

In addition, a 3-methoxy-4-hydroxy-styryl group was easily identified by $^1H-^1H$ COSY correlations of H-5′ (δ_H 6.83)/H-6′ (δ_H 6.84) and H-7′ (δ_H 6.41)/H-8′ (δ_H 5.92) and the HMBC correlations from H-2′ (δ_H 6.86) to C-4′ (δ_C 145.5), H-5′ (δ_H 6.83) to C-1′ (δ_C 129.2)/C-3′ (δ_C 146.5), H-6′ (δ_H 6.84) to C-2′ (δ_C 108.5)/C-4′ (δ_C 145.5), H-7′ (δ_H 6.41) to C-2′ (δ_C 108.5)/C-6′ (δ_C 120.1), and H-8′ (δ_H 5.92) to C-1′ (δ_C 129.2). Moreover, the $^1H-^1H$ COSY correlations of H-4 (δ_H 2.50, 2.62)/H-5 (δ_H 1.94, 2.01)/H-6 (δ_H 4.05)/H-7 (δ_H 3.31) and H-8 (δ_H 5.23)/H-9 (δ_H 2.37, 2.37)/H-10 (δ_H 1.51, 1.51)/H-11 (δ_H 0.96) and the HMBC correlations from H-4 (δ_H 2.50, 2.62) to C-3 (δ_C 148.5)/C-6 (δ_C 69.8)/C-7a (δ_C 125.6), H-5 (δ_H 1.94, 2.01) to C-3a (δ_C 151.1), H-6 (δ_H 4.05) to C-7a (δ_C 125.6), H-7 (δ_H 3.31) to C-5 (δ_C 25.5)/C-3a (δ_C 151.1)/C-1 (δ_C 169.0), H-8 (δ_H 5.23) to C-3a (δ_C 151.1)/C-10 (δ_C 22.4), and H-9 (δ_H 2.37, 2.37) to C-3 (δ_C 148.5)/C-11 (δ_C 13.9) indicated the presence of 6-hydroxylphthalide moiety. Furthermore, the $^1H-^1H$ COSY correlation of H-8′ (δ_H 5.92)/H-7 (δ_H 3.31) and HMBC correlations from H-8′ (δ_H 5.92) to C-6 (δ_C 69.8)/C-7a (δ_C 125.6), and H-7 (δ_H 3.31) to C-7′ (δ_C 133.3) suggested that the 3-methoxy-4-hydroxy-styryl group connects at C-7 of phthalide moiety (Figure 5). Thus, the planar structure of compound **4** was determined as a novel phthalide-phenylpropanoid heterodimer, and the assignments of all of the proton and carbon resonances are shown in Table 2.

Table 2. ^1H NMR (600 MHz) and ^{13}C NMR (150 MHz) data of 4 and 5 in $CDCl_3$ (δin ppm, J in Hz)

	4		5	
no.	δ_H	δ_C	δ_H	δ_C
1		169.0, C		167.6, C
3		148.5, C		148.1, C
4	2.62, m	17.8 CH_2	2.64, m	17.9, CH_2
	2.50, dt (18.4, 5.4)		2.53, dt (18.5, 5.8)	
5	2.01, m	25.5, CH_2	2.04, m	26.1, CH_2
	1.94, m			
6	4.05, m	69.8, CH	4.19, m	69.0, CH
7	3.31, dd (8.0, 4.3)	43.6, CH	5.63, d (4.2)	68.4, CH
8	5.23, t (7.9)	111.9, CH	5.35, t (7.9)	114.4, CH
9	2.37, m	28.0, CH_2	2.39, m	28.1, CH_2
10	1.51, m	22.4, CH_2	1.52, m	22.4, CH_2
11	0.96, t (7.4)	13.9, CH_3	0.96, t (7.6)	13.9, CH_2
3a		151.1, C		155.2, C
7a		125.6, C		122.3, C
1′		129.2, C		126.8, C
2′	6.86, br. s	108.5, CH	7.02, br. s	109.5, CH
3′		146.5, C		146.8, C
4′		145.5, C		148.3, C
5′	6.83, d (8.6)	114.4, CH	6.91, d (8.2)	114.8, CH
6′	6.84, br. d (8.6)	120.1, CH	7.07, br. d (8.2)	123.5, CH
7′	6.41, d (15.8)	133.3, CH	7.66, d (15.7)	146.6, CH
8′	5,92, dd (15.8, 8.0)	124.4, CH	6.29, d (15.7)	114.4, CH
9′				167.4, C
3′-OMe	3.83, s	55.9, CH_3	3.92, s	56.0, CH_3

The phthalide moiety of **4** was extremely similar to 6,7-dihydroxyligustilide derivatives, and the configuration of double bond (C-3−C-8) in **4** was determined as (*Z*)-form based on the chemical shift value of H-8 (δ_H 5.23). Previous research showed that the chemical shift values of H-8 of (*Z*)- and (*E*)-6,7-dihydroxyligustilide derivatives were about 5.30 and 5.80 ppm, respectively.[24,25] The relative configurations of

https://doi.org/10.1021/acsomega.3c06172
ACS Omega 2023, 8, 39855−39864

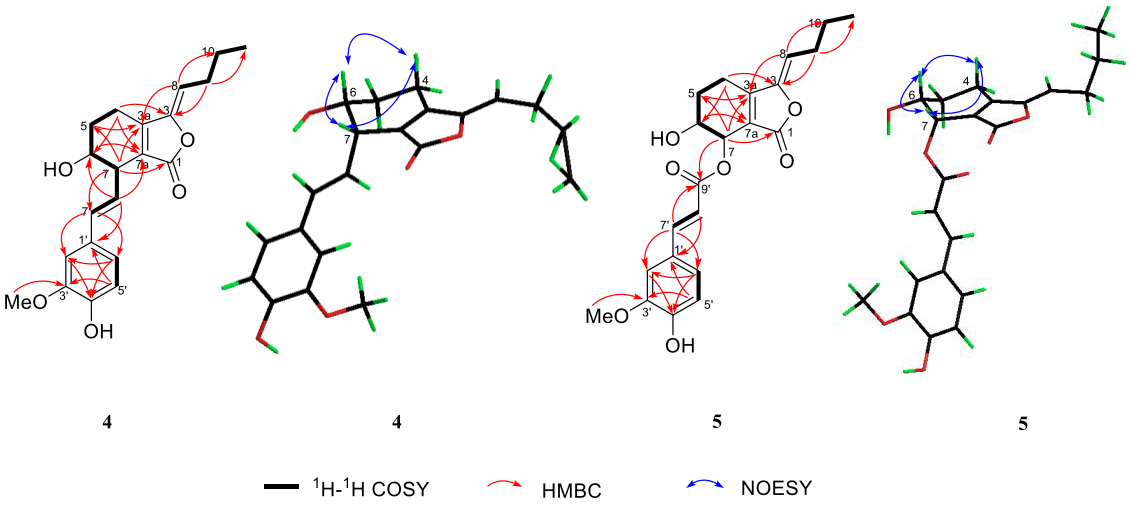

Figure 5. Key 2D NMR correlations of **4** and **5**.

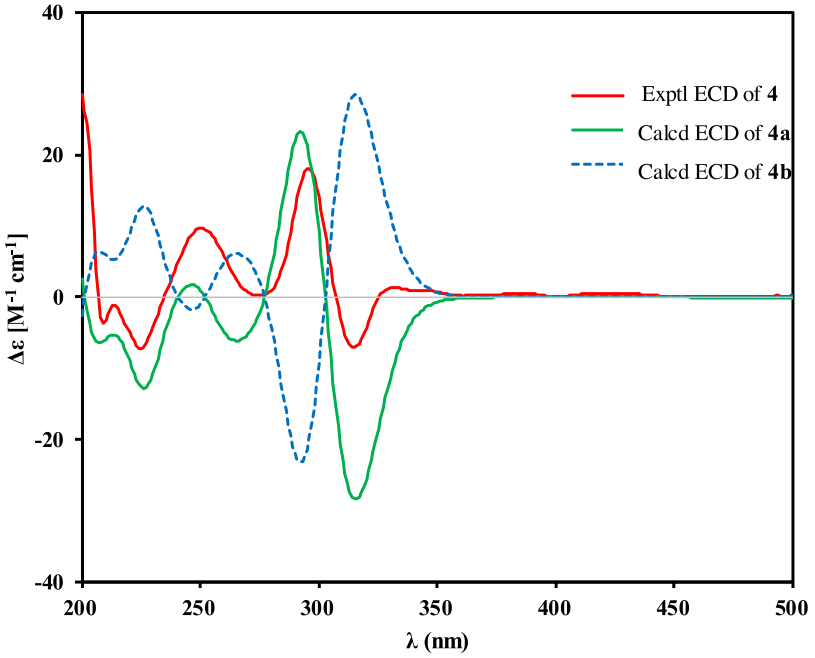

Figure 6. Comparison of the calculated ECD spectra for **4a** and **4b** with the experimental spectrum of **4**.

C-6 and C-7 of **4** were established on the basis of coupling constant analysis and correlations, and the relatively small coupling constant between H-6 and H-7 (J = 4.3 Hz) indicated the *cis* configuration of the two protons.[23] The deduction was also confirmed by the ROESY experiment. The ROESY correlations of H-6/H-7/H-4a (δ_H 2.62), indicated that H-6, H-7, and H-4a were located on the same face (Figure 5). As such, the relative configuration of **4** was assigned as 6*R**, 7*S**.

Finally, the absolute configuration of **4** was established by TDDFT quantum chemical calculations of its ECD spectrum on two possible structures: (6*R*, 7*S*)-**4** (**4a**) and (6*S*, 7*R*)-**4** (**4b**). As shown in Figure 6, the calculated weighted ECD spectrum of **4a** matched well with the experimental ECD, indicating the absolute configuration of **4** to be 6*R*, 7*S*.

Given that **4** bears a novel carbon skeleton, the calculations for the ^{13}C NMR chemical shifts of (6*R*,7*S*)-**4** (**4a**) were performed at the mPW1PW91/6-311+G(2d, p) level. The results showed that the correlation coefficient (R^2) between the calculated and experimental data from the linear regression analysis was 0.9980 (Figure 7), and the mean absolute deviation (MAD) was 1.98 ppm (Tables S10 and S11, Supporting Information), which provided further evidence for the structure of **4**.

Ligusticumalide B (**5**), obtained as a yellow oil, was assigned the molecular formula ($C_{22}H_{24}O_7$) based on the analysis of HR-ESIMS data (m/z 423.1405 [M + Na]$^+$, calcd. 423.1414). The NMR data of **5** were close to those of **4**, except that **5** had two oxygenated methines and an extra carbonyl carbon signal (δ_C 167.4). Further inspection of NMR data of **5** hinted that the structure of compound **5** was the ester formed by the condensation of senkyunolide H and ferulic acid.

The planar structure of compound **5** was further determined by the 2D NMR data. The ^{1}H−^{1}H COSY correlations of H-4 (δ_H 2.53, 2.64)/H-5 (δ_H 2.04, 2.04)/H-6 (δ_H 4.19)/H-7 (δ_H 5.63) and H-8 (δ_H 5.35)/H-9 (δ_H 2.39, 2.39)/H-10 (δ_H 1.52, 1.52)/H-11 (δ_H 0.96) and the HMBC correlations from H-4

https://doi.org/10.1021/acsomega.3c06172
ACS Omega 2023, 8, 39855−39864

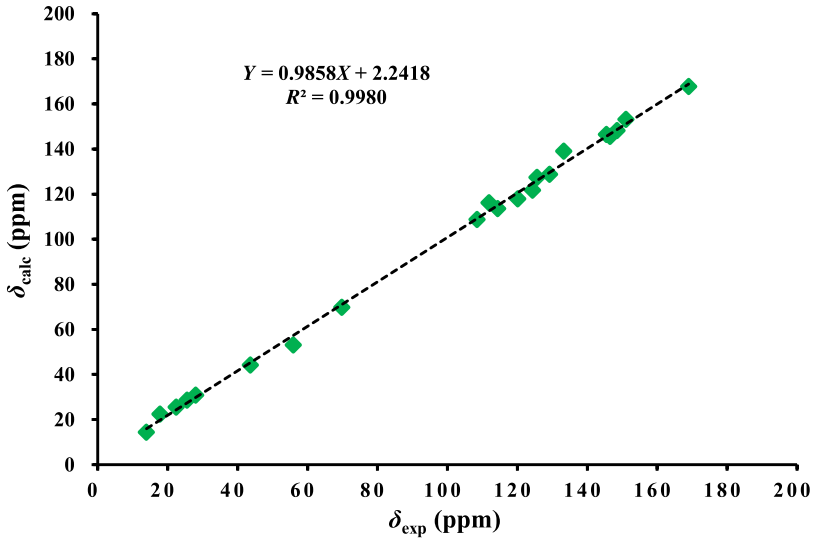

Figure 7. Regression analysis of experimental versus calculated ^{13}C NMR chemical shifts of **4**.

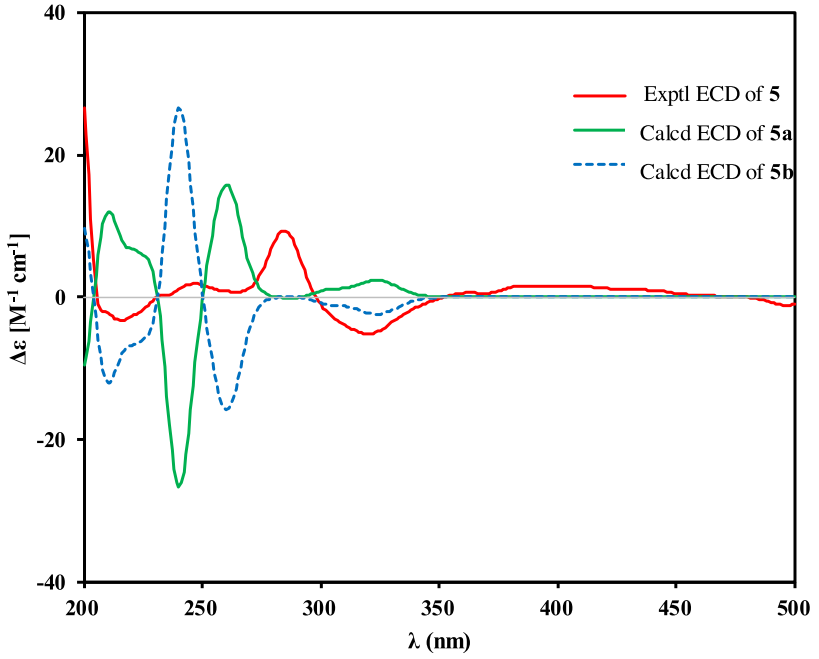

Figure 8. Comparison of the calculated ECD spectra for **5a** and **5b** with the experimental spectrum of **5**.

(δ_H 2.53, 2.64) to C-3 (δ_C 148.1)/C-6 (δ_C 69.0)/C-7a (δ_C 122.3), H-5 (δ_H 2.04, 2.04) to C-3a (δ_C 151.2), H-6 (δ_H 4.19) to C-7a (δ_C 122.3), H-7 (δ_H 5.63) to C-5 (δ_C 26.1)/C-3a (δ_C 151.2)/C-1 (δ_C 167.6), H-8 (δ_H 5.35) to C-3a (δ_C 155.2)/C-10 (δ_C 22.4), and H-9 (δ_H 2.39, 2.39) to C-3 (δ_C 148.1)/C-11 (δ_C 13.9) also indicated the presence of a 6-hydroxylphthalide part. Moreover, one feruloyl was confirmed based on the ^{1}H−^{1}H COSY correlations of H-5′ (δ_H 6.91)/H-6′ (δ_H 7.07) and H-7′ (δ_H 7.66)/H-8′ (δ_H 6.29) and the HMBC correlations from H-2′ (δ_H 7.02) to C-4′ (δ_C 148.3), H-5′ (δ_H 6.91) to C-1′ (δ_C 126.8)/C-3′ (δ_C 146.8), H-6′ (δ_H 7.07) to C-2′ (δ_C 109.5)/C-4′ (δ_C 148.3), H-7′ (δ_H 7.66) to C-2′ (δ_C 109.5)/C-6′ (δ_C 123.5)/C-9′ (δ_C 167.4), H-8′ (δ_H 6.29) to C-1′ (δ_C 126.8), and methoxy protons (δ_H 3.92) to C-3′ (δ_C 146.8). The HMBC correlation from H-7 (δ_H 5.63) to C-9′ (δ_C 167.4) revealed the feruloyl group connected at C-7 of the 6-hydroxylphthalide moiety. Thus, compound **5** was identified as a rare phthalide-phenylpropanoid heterodimer linked by C-7−O-C-9′ (Figure 5).

Additionally, the relative configuration of **5** was determined to be 6*R**, 7*S** based on analysis of the ROESY spectrum (5) and $J_{H\text{-}6,\,7}$ value (J = 4.2 Hz) (Table 2). Meanwhile, the double bond (C-3−C-8) of compound **5** was also assigned a (*Z*)-configuration by the same method as that used for compound **4**.

To establish the absolute configuration of **5**, the ECD spectra of the two possible structures (6*R*, 7*S*)-**5** (**5a**) and (6*S*, 7*R*)-**5** (**5b**) were calculated by TDDFT methods. As shown in Figure 8, the calculated ECD spectrum of (6*S*, 7*R*)-**5** (**5b**) matched well with the experimental one, defining the (6*S*, 7*R*) absolute configuration of **5**.

Structurally, compounds **1**−**3** represent a group of 8′−9-linked neolignans. In particular, lignan featuring a C-8′−C-9-linked skeleton is a rare occurrence in nature, with only around

https://doi.org/10.1021/acsomega.3c06172
ACS Omega 2023, 8, 39855−39864

50 examples of this chemotype reported in the literature.[26−29] Moreover, **1** is a novel 9-norneolignan containing a 7, 8′-epoxy tetrahydrofuran ring moiety, while **3** represents the fifth example of phenylpropanoid trimers with 8′-9-type neolignan skeleton.[28] Compounds **4** and **5** are novel phthalide-phenylpropanoid heterodimers, representing a new class of natural products. Notably, **4** possesses a 7-styryl phthalide skeleton, which is unreported and might derive from a nor-heterodimer of phthalide-phenylpropanoid.

2.2. XO Inhibitory Activities of 1−5. Considering that compounds **1−5** were obtained from the fractions of ethyl acetate extracts of *R. chuanxiong* with XO inhibitory activity, these isolates were evaluated for their *anti*-XO activities *in vitro*. The results suggested that four compounds (**1−3** and **5**) exhibited moderate inhibitory activities against XO and had inhibitory rates of 43.92%, 31.06%, 49.28%, and 40.28% at the concentration of 500.00 μM, respectively. It is worth mentioning that compound **4**, with the nor-carbon hybrid skeleton of phthalide and phenylpropanoid, showed better activity of inhibiting the XO with the inhibitory rate of 99.49% (500.00 μM) and further investigation on the concentration−inhibitory effect relationship revealed that the IC_{50} value of **4** was 93.88 μM (Table 3).

Table 3. Inhibition of Compounds 1−5 on the XO

compounds	inhibitory rates (%)[a]	IC_{50} (μM)
1	43.92	>500
2	31.06	>500
3	49.28	>500
4	99.49	93.88
5	40.28	>500
allopurinol[b]	99.98	3.40

[a]The sample concentration is 500 μM. [b]Allopurinol, an *anti*-XO agent used as the positive control.

3. CONCLUSIONS

In summary, chemical investigations on ethyl acetate extracts of *R. chuanxiong*, which showed potent antigout effects *in vivo*, were carried out, resulting in the isolation of three rare 8′, 9-linked neolignans (ligusticumins A−C) and two novel phthalide-phenylpropanoid heterodimers (ligusticumalides A−B). Among them, ligusticumalide A has an unreported 7-styryl phthalide skeleton. Their structures were unambiguously determined *via* extensive spectroscopic analyses in combination with computational approaches. The bioassay results suggested that **4** showed significant inhibitory activity against XO with an IC_{50} value of 93.88 μM.

4. EXPERIMENTAL SECTION

4.1. General Experimental Procedures. Optical rotations were tested on a Jasco model 1020 digital polarimeter (Horiba, Tokyo, Japan). The ECD data were measured on a Chirascan spectropolarimeter (Applied Photophysics, Leatherhead, U.K.). 1D and 2D NMR spectra were recorded on a Bruker AVANCE III-600 spectrometer (Bruker, Bremerhaven, Germany). HR-ESIMS were executed on a hybrid quadrupole-TOF mass spectrometer (Triple TOF 5600+, AB Sciex, Framingham, MA).

4.2. Plant Material. The *R. chuanxiong* was purchased from Shaanxi Sciendan Pharmaceutical Co., Ltd. Tongchuan City, Shaanxi Province, China, and the sample was authenticated by Dr. Hongbo Xu (Shaanxi University of Chinese Medicine, China). A voucher specimen (No. 20200201) was deposited in the Laboratory of Shaanxi Collaborative Innovation Center of Chinese Medicinal Resources Industrialization (Shaanxi University of Chinese Medicine).

4.3. Extraction and Isolation. The air-dried and powdered *R. chuanxiong* (5 kg) was ultrasonically extracted twice with ethyl acetate (1 h at a time). The extract was evaporated under reduced pressure to give the EtOAc extract (290 g). The EtOAc part (280 g) was loaded to macroporous resin column chromatography and sequentially eluted with water, 50% methanol, and methanol to afford three fractions: Frs. A−C. Fr. C (120 g) was subjected to silica gel column chromatography (SiCC) (2 kg, 18 × 150 cm^2) with a stepwise gradient of ethyl acetate-petroleum ether (*v*/*v*, 0:100−100:0) to afford ten fractions (Frs. C-1−C-10). Fr. C-8 (8.9 g) was loaded to SiCC (100 g, 2 × 50 cm^2) with a gradient solvent system of acetone-petroleum ether (*v*/*v*, 10:90−100:0) to obtain 14 subfractions (Frs. C-8−1−C-8−14). Fr. C-8−8 (50 mg) was further isolated by prep-HPLC (YMC-Pack ODS-A, 5 μm, 250 × 10 mm^2, 3 mL/min) to yield compounds **2** (1.0 mg), **4** (2.0 mg), and **5** (2.1 mg). Fr. C-8−9 (100 mg) was subjected to Sephadex LH-20 column chromatography (100 g, 2 × 150 cm^2) using methanol as the eluent to give Fr. C-8−9−1 and Fr. C-8−9−2. The two subfractions were respectively purified by prep-HPLC (YMC-Pack ODS-A, 5 μm, 250 × 10 mm^2, 3 mL/min) to yield compounds **3** (16.0 mg) and **1** (1.1 mg).

4.3.1. Ligusticumin A (1). $[\alpha]_D^{29}$ +385.4 (*c* 0.065, MeOH); ECD (*c* 40 μM, MeOH): λ_{max} ($\Delta\varepsilon$) 209 (+20.1), 225 (+27.1), 245 (−27.5), 265 (−15.3) nm; ^{1}H and ^{13}C NMR data see Table 1; HR-ESIMS (+) *m*/*z* 399.1412 $[M + Na]^+$ (calcd for $C_{20}H_{24}O_7Na$, 399.1414).

4.3.2. Ligusticumin B (2). $[\alpha]_D^{29}$ + 255.4 (*c* 0.065, MeOH); ECD (c 40 μM, MeOH): λ_{max} ($\Delta\varepsilon$) 209 (−2.4), 218 (−9.6), 232 (+2.1), 275 (+13.4), 290 (+14.4), 330 (+10.1), 359 (−3.5), 387 (+7.3), 416 (−2.3) nm; ^{1}H and ^{13}C NMR data see Table 1; HR-ESIMS (+) *m*/*z* 411.1409 $[M + Na]^+$ (calcd for $C_{21}H_{24}O_7Na$, 411.1414).

4.3.3. Ligusticumin C (3). $[\alpha]_D^{29}$ +139.2 (*c* 0.065, MeOH); ECD (*c* 40 μM, MeOH): λ_{max} ($\Delta\varepsilon$) 210 (−12.2), 223 (−14.0), 247 (+5.6), 262 (+3.6), 295 (+11.7), 321 (+3.0), 360 (−3.8), 403 (+8.1), 425 (−4.7) nm; ^{1}H and ^{13}C NMR data see Table 1; HR-ESIMS (+) *m*/*z* 573.2086 $[M + Na]^+$ (calcd for $C_{31}H_{34}O_9Na$, 573.2095).

4.3.4. Ligusticumalide A (4). $[\alpha]_D^{29}$ +322.1 (*c* 0.065, MeOH); ECD (c 40 μM, MeOH): λ_{max} ($\Delta\varepsilon$) 209 (−3.6), 225 (−7.2), 250 (+9.8), 297 (+17.8), 315 (−7.1) nm; ^{1}H and ^{13}C NMR data see Table 2; HR-ESIMS (+) *m*/*z* 357.1699 $[M + Na]^+$ (calcd for $C_{21}H_{24}O_5Na$, 357.1697).

4.3.5. Ligusticumalide B (5). $[\alpha]_D^{29}$ +208.3 (*c* 0.065, MeOH); ECD (c 40 μM, MeOH): λ_{max} ($\Delta\varepsilon$) 208 (−1.9), 218 (−3.1), 243 (+1.7), 267 (+0.3), 285 (+9.4), 320 (−5.2) nm; ^{1}H and ^{13}C NMR data see Table 2; HR-ESIMS (+) *m*/*z* 423.1405 $[M + Na]^+$ (calcd for $C_{21}H_{24}O_5Na$, 423.1414).

4.4. ECD Calculations. The conformation analyses were performed utilizing the molecular mechanics MMFF94s implemented in Spartan′14 (Wave function Inc., Irvine, CA). Conformers exhibiting populations exceeding 1% were subjected to optimization using the HF/6-311G (d, p) method and subsequently further refined using the density functional theory (DFT) method at the B3LYP/6-311G (d, p) level

https://doi.org/10.1021/acsomega.3c06172
ACS Omega 2023, 8, 39855−39864

within the Gaussian program[30] (Supporting Information). The stability of the optimized conformers was confirmed by calculating their free energies and vibrational frequencies at the aforementioned level, and no imaginary frequencies were detected. The TDDFT/B3LYP/6-311+G (2d, p) method was employed to compute the energies, oscillator strengths, and rotational strengths (velocity) of the first 30 electronic excitations. The calculated ECD data for these conformers were averaged based on the principles of the Boltzmann distribution theory.

4.5. ^{13}C NMR Calculations. The conformations generated by Spartan′14 were subjected to optimization in the gas phase at the B3LYP/6-31+G (d, p) level using the Gaussian program. Subsequently, the ^{13}C NMR chemical shifts of the optimized conformers were computed using the GIAO method at the mPW1PW91/6-311+G (2d, p) level in MeOH, employing an IEFPCM model (Supporting Information). The calculated NMR data were averaged based on the principles of the Boltzmann distribution theory, in which the values of the linear correlation coefficient (R^2) and mean absolute deviation (MAD) were determined to evaluate the results.[30]

4.6. XO Inhibition Assays. The XO inhibitory activities were evaluated using a spectrophotometric method with xanthine as the substrate, following the procedure described in our previous research.[31] In brief, the assay mixture consisted of 20 μL of the test solution, 80 μL of phosphate buffer (pH 7.5), and 50 μL of enzyme solution (0.1 units/mL in phosphate buffer, pH 7.5). After preincubation at 37 °C for 5 min, the reaction was initiated by adding 50 μL of substrate solution (150 μM xanthine in the same buffer). The assay mixture was further incubated at 37 °C for 3 min.

The formation of uric acid, indicated by the increase in absorbance at 295 nm, was measured using a Multiskan Go spectrophotometer (Thermo Scientific, NH). Allopurinol was employed as a positive control to validate the reliability of the enzyme assay. Each test concentration was tested twice, and IC_{50} values were determined based on the mean values obtained from two independent experiments.

■ ASSOCIATED CONTENT

Supporting Information

The Supporting Information is available free of charge at https://pubs.acs.org/doi/10.1021/acsomega.3c06172.

HR-ESIMS, NMR data, and the calculation details of compounds **1**−**5** (PDF)

■ AUTHOR INFORMATION

Corresponding Authors

Zhi-Shu Tang − *Shaanxi Collaborative Innovation Center of Chinese Medicine Resources Industrialization, State Key Laboratory of Research & Development of Characteristic Qin Medicine Resources (Cultivation), Shaanxi Innovative Drug Research Center, Shaanxi University of Chinese Medicine, Xianyang 712046, People's Republic of China; China Academy of Chinese Medical Sciences, Beijing 100700, People's Republic of China*; Phone: +86 (0)29 3818 2202; Email: tzs6565@163.com; Fax: +86 (0)29 3818 2201

Hong-Bo Xu − *Shaanxi Collaborative Innovation Center of Chinese Medicine Resources Industrialization, State Key Laboratory of Research & Development of Characteristic Qin Medicine Resources (Cultivation), Shaanxi Innovative Drug Research Center, Shaanxi University of Chinese Medicine, Xianyang 712046, People's Republic of China*; orcid.org/0000-0001-9633-5566; Email: xhb2005@sntcm.edu.cn

Authors

Man-Li Yang − *Nanjing University of Chinese Medicine, Nanjing 210023, People's Republic of China*

Hao-Dong Yang − *Shaanxi Collaborative Innovation Center of Chinese Medicine Resources Industrialization, State Key Laboratory of Research & Development of Characteristic Qin Medicine Resources (Cultivation), Shaanxi Innovative Drug Research Center, Shaanxi University of Chinese Medicine, Xianyang 712046, People's Republic of China*

Xiao-Hui Hu − *Shaanxi Collaborative Innovation Center of Chinese Medicine Resources Industrialization, State Key Laboratory of Research & Development of Characteristic Qin Medicine Resources (Cultivation), Shaanxi Innovative Drug Research Center, Shaanxi University of Chinese Medicine, Xianyang 712046, People's Republic of China*

Rui Zhou − *Shaanxi Collaborative Innovation Center of Chinese Medicine Resources Industrialization, State Key Laboratory of Research & Development of Characteristic Qin Medicine Resources (Cultivation), Shaanxi Innovative Drug Research Center, Shaanxi University of Chinese Medicine, Xianyang 712046, People's Republic of China*

Tao-Tao Xue − *Shaanxi Collaborative Innovation Center of Chinese Medicine Resources Industrialization, State Key Laboratory of Research & Development of Characteristic Qin Medicine Resources (Cultivation), Shaanxi Innovative Drug Research Center, Shaanxi University of Chinese Medicine, Xianyang 712046, People's Republic of China*; orcid.org/0009-0002-0964-9802

Kang Ma − *Shaanxi Collaborative Innovation Center of Chinese Medicine Resources Industrialization, State Key Laboratory of Research & Development of Characteristic Qin Medicine Resources (Cultivation), Shaanxi Innovative Drug Research Center, Shaanxi University of Chinese Medicine, Xianyang 712046, People's Republic of China*

Chun Ji − *Shaanxi Collaborative Innovation Center of Chinese Medicine Resources Industrialization, State Key Laboratory of Research & Development of Characteristic Qin Medicine Resources (Cultivation), Shaanxi Innovative Drug Research Center, Shaanxi University of Chinese Medicine, Xianyang 712046, People's Republic of China*

Complete contact information is available at: https://pubs.acs.org/10.1021/acsomega.3c06172

Notes

The authors declare no competing financial interest.

■ ACKNOWLEDGMENTS

This work was supported by the program "Double Chain Integration" of the Young and Middle-aged Scientific Research Innovation Team Project of Shaanxi Provincial Administration of Traditional Chinese Medicine (2022-SLRH-YQ-005), the Shaanxi Youth Science and Technology New Star Project (2020KJXX-069), and the Shaanxi Provincial Key Research and Development Program (2023-ZDLSF-54).

■ REFERENCES

(1) Chen, Z.; Pan, X. K.; Georgakilas, A. G.; Chen, P.; Hu, H.; Yang, Y.; Tian, S. J.; Xia, L.; Zhang, J.; Cai, X. X.; et al. Tetramethylpyrazine (TMP) protects cerebral neurocytes and inhibits glioma by down

regulating chemokine receptor CXCR4 expression. *Cancer Lett.* **2013**, *336*, 281−289.
(2) Su, Y. L.; Fu, Z. Y.; Quan, C. J.; Wang, W. M. Fabrication of nano *Rhizama Chuanxiong* particles and determination of tetramethylpyrazine. *Trans. Nonferrous Met. Soc. China* **2006**, *16*, s393−s397.
(3) Hu, X. H. *Study on the Anti-Gout Active Components of Traditional Chinese Medicine Ligusticum Chuanxiong Based on Xanthine Oxidase Target*; Shaanxi University of Chinese Medicine: Xianyang, China, 2022.
(4) Li, D.; Long, Y.; Yu, S.; Shi, A.; Wan, J. Y.; Wen, J.; Li, X. Q.; Liu, S. Y.; Zhang, Y. L.; Li, N.; et al. Research advances in cardio-cerebrovascular diseases of *Ligusticum chuanxiong* Hort. *Front. Pharmacol.* **2022**, *12*, No. 832673.
(5) Ran, X.; Ma, L.; Peng, C.; Zhang, H.; Qin, L. P. *Ligusticum chuanxiong* Hort: a review of chemistry and pharmacology. *Pharm. Biol.* **2011**, *49*, 1180−1189.
(6) Tang, Z. Z.; Qin, Y. H.; Chen, W. H.; Zhao, Z. Q.; Lin, W. J.; Xiao, Y. R.; Chen, H.; Liu, Y. T.; Chen, H.; Bu, T. L.; et al. Diversity, chemical constituents, and biological activities of endophytic fungi isolated from *Ligusticum chuanxiong* Hort. *Front. Microbiol.* **2021**, *12*, No. 771000.
(7) Yang, C. L. H.; Or, T. C. T.; Lau, J. S. H.; Lau, A. S. Y. *Ligusticum chuanxiong* and its decoctions: Effects and underlying mechanisms of action on stroke. *Adv. Bot. Res.* **2012**, *62*, 315−341.
(8) Shi, C.; Zhou, Z.; Chi, X.; Xiu, S.; Yi, C.; Jiang, Z.; Chen, R.; Zhang, L.; Liu, Z. Recent advances in gout drugs. *Eur. J. Med. Chem.* **2023**, *245*, No. 114890.
(9) Endrini, S.; Bakar, F. I. A.; Bakar, M. F. A.; Abdullah, N.; Marsiati, H. Phytochemical profiling, *in vitro* and *in vivo* xanthine oxidase inhibition and antihyperuricemic activity of Christia vespertilionis leaf. *Biocatal. Agric. Biotechnol.* **2023**, *48*, No. 102645.
(10) Scanu, A.; Luisetto, R.; Ramonda, R.; Spinella, P.; Sfriso, P.; Galozzi, P.; Oliviero, F. Anti-Inflammatory and Hypouricemic Effect of Bioactive Compounds: Molecular Evidence and Potential Application in the Management of Gout. *Curr. Issues Mol. Biol.* **2022**, *44*, 5173−5190.
(11) Moubarez, D. A. The predictive value of serum uric acid in development of acute kidney injury and mortality in patients with sepsis. *J. Nephropathol.* **2022**, *11*, No. e17307, DOI: 10.34172/jnp.2022.17307.
(12) Kuwabara, M.; Kodama, T.; Ae, R.; Kanbay, M.; Andres-Hernando, A.; Borghi, C.; Hisatome, I.; Lanaspa, M. A. Update in uric acid, hypertension, and cardiovascular diseases. *Hypertens. Res.* **2023**, *46*, 1714−1726, DOI: 10.1038/s41440-023-01273-3.
(13) Harrold, L. R.; Andrade, S. E.; Briesacher, B. A.; Raebel, M. A.; Fouayzi, H.; Yood, R. A.; Ockene, I. S. Adherence with urate-lowering therapies for the treatment of gout. *Arthritis Res. Ther.* **2009**, *11*, No. R46, DOI: 10.1186/ar2659.
(14) Dawson, J.; Walters, M. Uric acid and xanthine oxidase: future therapeutic targets in the prevention of cardiovascular disease? *Br. J. Clin. Pharmacol.* **2006**, *62*, 633−644.
(15) Grewal, H. K.; Martinez, J. R.; Espinoza, L. R. Febuxostat: drug review and update. *Expert Opin. Drug Metab. Toxicol.* **2014**, *10*, 747−758.
(16) Šmelcerović, A.; Tomović, K.; Šmelcerović, Ž.; Petronijević, Ž.; Kocić, G.; Tomašič, T.; Jakopin, Ž.; Anderluh, M. Xanthine oxidase inhibitors beyond allopurinol and febuxostat; an overview and selection of potential leads based on in silico calculated physico-chemical properties, predicted pharmacokinetics and toxicity. *Eur. J. Med. Chem.* **2017**, *135*, 491−516.
(17) Xu, H. B.; Zhou, R.; Xie, P.; Song, Z. X.; Liu, L.; Lei, H.; Tang, Z. S. Xanthine oxidase inhibitory activity of 27 Chinese medicinal plants. *Lishizhen Med. Mater. Med. Res.* **2017**, *28*, 547−548.
(18) Wang, H.; Zhang, H. W.; Zhang, X. M.; Yin, Y. C.; Ding, G. Q.; Tang, X. W.; Hou, P. Y.; Sun, S. W.; Wang, W. Identification of coniferyl ferulate as the bioactive compound behind the xanthine oxidase inhibitory activity of *Chuanxiong Rhizome*. *J. Funct. Foods* **2023**, *100*, No. 105378.
(19) Hong-Bo, X.; Zhi-Shu, T.; Rui, Z.; Xiao-Hui, H.; Kang, M. Application of the active part of *Rhizoma Chuanxiong* in the preparation of anti-gout medicine. 2023.
(20) Wang, H.; Geng, C. A.; Xu, H. B.; Huang, X. Y.; Ma, Y. B.; Yang, C. Y.; Zhang, X. M.; Chen, J. J. Lignans from the fruits of *Melia toosendan* and their agonistic activities on melatonin receptor MT1. *Planta Med.* **2015**, *81*, 847−854.
(21) Li, L.; Seeram, N. P. Further investigation into maple syrup yields 3 new lignans, a new phenylpropanoid, and 26 other phytochemicals. *J. Agric. Food Chem.* **2011**, *59*, 7708−7716.
(22) Deyama, T.; Ikawa, T.; Kitagawa, S.; Nishibe, S. The constituents of Eucommia ulmoides OLIV. III.: Isolation and structure of a new lignan glycoside. *Chem. Pharm. Bull.* **1986**, *34*, 523−527.
(23) Naito, T.; Katsuhara, T.; Niitsu, K.; Ikeya, Y.; Okada, M.; Mitsuhashi, H. Two phthalides from *Ligusticum chuangxiong*. *Phytochemistry* **1992**, *31*, 639−642.
(24) Lu, X. H.; Liang, H.; Zhao, Y. Y. Isolation and indentification of the ligustilide compounds from the root of *Angelica sinensis*. *China J. Chin. Mater. Med.* **2003**, *5*, 43−45.
(25) Zuo, A. H.; Cheng, M. C.; Zhuo, R. J.; Wang, L.; Xiao, H. B. Structure elucidation of degradation products of Z-ligustilide by UPLC-QTOF-MS and NMR spectroscopy. *Acta Pharm. Sin.* **2013**, *48*, 911−916.
(26) Ma, X. N.; Xie, C. L.; Miao, Z.; Yang, Q.; Yang, X. W. An overview of chemical constituents from *Alpinia* species in the last six decades. *RSC Adv.* **2017**, *7*, 14114−14144.
(27) Teponno, R. B.; Kusari, S.; Spiteller, M. Recent advances in research on lignans and neolignans. *Nat. Prod. Rep.* **2016**, *33*, 1044−1092.
(28) Wan, S. J.; Ren, H. G.; Jiang, J. M.; Xu, G.; Xu, Y.; Chen, S. M.; Chen, G.; Zheng, D.; Yuan, M.; Zhang, H.; Xu, H. X. Two novel phenylpropanoid trimers From *Ligusticum chuanxiong* Hort with inhibitory activities on alpha-hemolysin secreted by *Staphylococcus aureus*. *Front. Chem.* **2022**, *10*, No. 877469.
(29) Cheng, Z. B.; Lu, X.; Bao, J. M.; Han, Q. H.; Dong, Z.; Tang, G. H.; Gan, L. S.; Luo, H. B.; Yin, S. (±)-Torreyunlignans A−D, rare 8−9′ linked neolignan enantiomers as phosphodiesterase-9A inhibitors from *Torreya yunnanensis*. *J. Nat. Prod.* **2014**, *77*, 2651−2657.
(30) Xu, H. B.; Yang, T. H.; Xie, P.; Tang, Z. S.; Xu, H. L.; Deng, C.; Liang, Y. N.; Zhou, R.; Liu, S. J.; Zhang, Y. Cyperane-type and related (nor) sesquiterpenoids from the root bark of *Acanthopanax gracilistylus* and their inhibitory effects on nitric oxide production. *J. Nat. Prod.* **2020**, *83*, 1453−1460.
(31) Xu, H. B.; Yang, T. H.; Xie, P.; Liu, S. J.; Liang, Y. N.; Zhang, Y.; Song, Z. X.; Tang, Z. S. Pheophytin analogues from the medicinal lichen *Usnea diffracta*. *Nat. Prod. Res.* **2018**, *32*, 1088−1094.

https://doi.org/10.1021/acsomega.3c06172
ACS Omega 2023, 8, 39855−39864